POTENTIAL ENERGY SURFACES CALCULATED USING MACROSCOPIC–MICROSCOPIC METHOD WITH THE LSD MODEL* **

J. Dudek

Institut de Recherches Subatomiques and Université Louis Pasteur
F-67037 Strasbourg Cedex 2, France

K. Mazurek and B. Nerlo-Pomorska

Institute of Theoretical Physics, Maria Curie-Skłodowska University
Pl. M. Curie-Skłodowskiej 1, 20-031 Lublin, Polska

(Received February 4, 2004)

A very accurate knowledge of the fission barrier shapes is necessary to predict the spontaneous fission life times of nuclei. Using the Strutinsky macroscopic–microscopic method we have performed calculations of the potential energy for even–even transuranic nuclei. The shell and pairing corrections are evaluated using the single-particle energies of the relativistic Woods–Saxon potential [1]. The microscopic corrections are added to the macroscopic energy obtained with the Lublin Strasburg Drop (LSD) model [2] to obtain the total potential energy in the multidimensional space of deformation parameters.

PACS numbers: 21.30.Fe, 21.60.–n, 71.10.Li

1. Introduction

The potential energy of a nucleus in the macroscopic–microscopic method is given by the sum

$$E_{\rm tot}(Z,N;{\rm def}) = E_{\rm LSD}(Z,N;{\rm def}) + E_{\rm micr}(Z,N;{\rm def})\,, \qquad (1)$$

in our approach the macroscopic term is represented by the Lublin Strasbourg Drop (LSD) formula, Ref. [2], which reproduces the masses of 2766

* Presented at the XXVIII Mazurian Lakes School of Physics, Krzyże, Poland, August 31–September 7, 2003.

** This work has been partly supported by the IN2P3-Polish Laboratories Convention under contract No. 99–95.

nuclei with the mean square deviation of 0.698 MeV when the deformation, shell and pairing corrections of Ref. [3] are included. It is interesting to examine the influence of the new liquid drop model and the single particle level scheme, obtained by the diagonalisation of the new relativistic Woods Saxon Hamiltonian, Ref. [1] and the exact treatment of the pairing force on the potential energy surfaces necessary to calculate the spontaneous fission half-lifes of nuclei. The LSD macroscopic energy is

$$\begin{aligned} E_{\rm LSD} &= ZM_H + NM_n - 0.00001433Z^{2.39} - b_{\rm vol}(1-\kappa_{\rm vol}I^2)A \\ &\quad + b_{\rm surf}(1-\kappa_{\rm surf}I^2)A^{2/3}B_{\rm surf}({\rm def}) \\ &\quad + b_{\rm curv}(1-\kappa_{\rm curv}I^2)A^{1/3}B_{\rm curv}({\rm def}) \\ &\quad + \frac{3}{5}e^2\frac{Z^2}{r_0^{\rm ch}A^{1/3}}B_{\rm Coul}({\rm def}) - C_4\frac{Z^2}{A} - 10\,\exp\left(-42\frac{|I|}{10}\right), \end{aligned} \tag{2}$$

where the parameters are

$$\begin{aligned} b_{\rm vol} &= 15.4920\ {\rm MeV}, & \kappa_{\rm vol} &= 1.8601, \\ b_{\rm surf} &= 16.9707\ {\rm MeV}, & \kappa_{\rm surf} &= 2.2938, \\ b_{\rm curv} &= 3.8602\ {\rm MeV}, & \kappa_{\rm curv} &= -2.3764, \\ r_0 &= 1.21725\,{\rm fm}, & C_4 &= 0.91810\ {\rm MeV}. \end{aligned}$$

The surface, curvature and Coulomb terms depend on the deformation. We have chosen the standard description of the nuclear shapes

$$\mathcal{R}(\theta,\phi) = R_0 c(\{\alpha_{\lambda,\mu}\})\left(1 + \sum_{\lambda=2}^{\lambda_{\rm max}}\sum_{\mu=-\lambda}^{\lambda}\alpha_{\lambda,\mu}Y_{\lambda,\mu}(\theta,\phi)\right), \tag{3}$$

where $Y_{\lambda,\mu}$ are the spherical harmonics and $c(\{\alpha_{\lambda\mu}\})$ ensures the volume conservation condition. The surface term contains the function

$$B_{\rm surf}({\rm def}) = \frac{S({\rm def})}{S(0)}, \tag{4}$$

where the surface of a deformed nucleus is

$$S({\rm def}) = \int_0^{2\pi}\int_0^{\pi} d\theta d\phi\ \ \mathcal{R}(\theta,\phi)\sqrt{[\mathcal{R}_\theta^2(\theta,\phi) + \mathcal{R}^2(\theta,\phi)]\sin^2\theta + \mathcal{R}_\phi^2(\theta,\phi)}\,; \tag{5}$$

$\mathcal{R}_\phi$ and $\mathcal{R}_\theta$ are the partial derivatives of $\mathcal{R}$. In the curvature term we have

$$B_{\rm curv}({\rm def}) = \frac{C({\rm def})}{C(0)}, \tag{6}$$

where the average-curvature term is

$$C(\mathrm{def}) = \frac{1}{2}\int_0^{2\pi}\int_0^{\pi} d\theta d\phi \;\; \mathcal{R}(\theta,\phi)\sqrt{[\mathcal{R}_\theta^2(\theta,\phi)+\mathcal{R}^2(\theta,\phi)]\sin^2\theta+\mathcal{R}_\phi^2(\theta,\phi)} \times\Big(\frac{1}{R_1(\theta,\phi)}+\frac{1}{R_2(\theta,\phi)}\Big)\,, \tag{7}$$

and where R_1 and R_2 are the principal curvature radii. Obviously the Coulomb energy depends also on the nuclear shape; we write in a standard way

$$B_{\mathrm{Coul}}(\mathrm{def}) = \frac{E_{\mathrm{Coul}}(\mathrm{def})}{E_{\mathrm{Coul}}(0)}\,, \tag{8}$$

where

$$\begin{aligned} E_{\mathrm{Coul}}(\mathrm{def}) &= \frac{1}{2}\int_{\nu'}\int_{\nu}\frac{\rho(\vec{r})\rho\,'(\vec{r}\,')}{|\vec{r}-\vec{r}\,'|}d^3\vec{r}\,d^3\vec{r}\,' \\ &= -\frac{1}{12}\rho_0^2\int_{S'_\nu}\int_{S_\nu}\frac{[(\vec{r}-\vec{r}\,')\cdot d\vec{S}][(\vec{r}-\vec{r}\,')\cdot d\vec{S}\,']}{|\vec{r}-\vec{r}\,'|}\,, \end{aligned} \tag{9}$$

ρ are the charge density distributions, ρ_0 the uniform one.

The microscopic part of (1) consists of the shell and pairing energies. The shell corrections are calculated within the Strutinsky method [4]. The pairing energy consists of the BCS [5] energy, projection correction and the average pairing terms. The parameters of these expressions are optimised using the single particle levels scheme of Woods–Saxon Hamiltonian.

In order to see better the role of different multipolarities on the barrier heights, we have performed the minimization of the potential energy with respect to the three different sets of deformation parameters: $\{\alpha_{20},\alpha_{22},\alpha_{40}\}$, $\{\alpha_{20},\alpha_{22},\alpha_{40},\alpha_{42},\alpha_{44}\}$ and $\{\alpha_{20},\alpha_{40},\alpha_{60}\}$. Here we focus on the comparison between the first two sets only. In Fig. 1, the ^{250}Cf path to fission found by minimization of the total energy with respect to $\{\alpha_{20},\alpha_{22},\alpha_{40},\alpha_{42},\alpha_{44}\}$ is drawn (solid line) and compared with the path to fission obtained in $\{\alpha_{20},\alpha_{22},\alpha_{40}\}$ space of deformation parameters (dashed line). In this particular nucleus the quadrupole non-axialities remain small (in comparison with $\gamma = 0$ dotted line), but this is by far not a general rule; this effect combined with the coupling to the hexadecapole non-axialities (α_{42}) will be discussed in detail elsewhere.

The (x,y)-coordinates are connected with $\{\alpha_{20},\alpha_{22}\}$ by the expressions

$$x = \beta\cos(\gamma+30^\circ)\,, \quad y = \beta\sin(\gamma+30^\circ)\,, \tag{10}$$

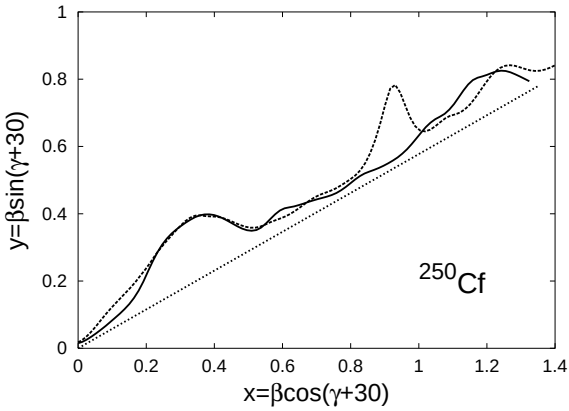

Fig. 1. Path to fission found by minimization of the total energy with respect to $\{\alpha_{20}, \alpha_{22}, \alpha_{40}, \alpha_{42}, \alpha_{44}\}$ (solid line) and $\{\alpha_{20}, \alpha_{22}, \alpha_{40}\}$ (dashed line) for ^{250}Cf; for reference also $\gamma = 0$ line (stright dotted line) is drawn.

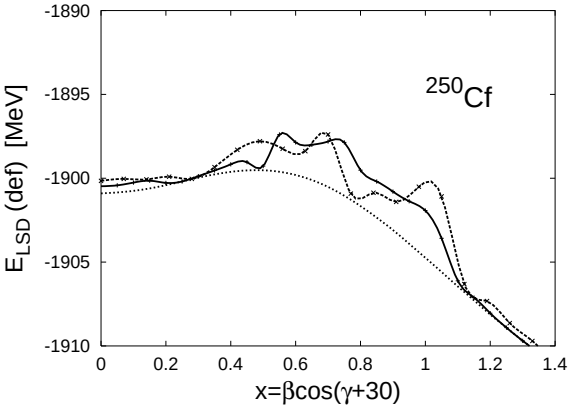

Fig. 2. Macroscopic energy obtained along the fission path with the sets of deformation parameters $\{\alpha_{20}, \alpha_{22}, \alpha_{40}, \alpha_{42}, \alpha_{44}\}$ (solid line) and $\{\alpha_{20}, \alpha_{22}, \alpha_{40}\}$ (dashed line), compared with the LSD model, minimal macroscopic energy $E^{\min}_{\rm LSD}$ $\{\alpha_{20}, \alpha_{22}, \alpha_{40}, \alpha_{42}, \alpha_{44}\}$ (dotted line), crosses denote the x grid points.

where

$$\alpha_{20} = \beta\cos(\gamma) \;\text{ and }\; \alpha_{22} = \frac{1}{\sqrt{2}}\beta\sin(\gamma)\,. \tag{11}$$

In Fig. 2 the macroscopic LSD energy of ^{250}Cf is drawn along the two non-axial paths to fission. In Fig. 3 the microscopic energies of ^{250}Cf along the path to fission found with (solid line) and without (dashed line) nonaxial degrees of freedom are drawn.

In Fig. 4 the total energy minus $E_{\rm LSD}(0)$ of ^{250}Cf along the both paths to fission is shown.

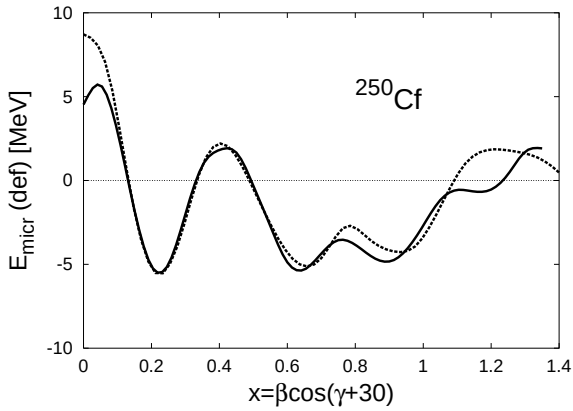

Fig. 3. Comparison of the microscopic energy obtained along fission path with deformation parameters $\{\alpha_{20}, \alpha_{22}, \alpha_{40}, \alpha_{42}, \alpha_{44}\}$ (solid line) and $\{\alpha_{20}, \alpha_{22}, \alpha_{40}\}$ (dashed line).

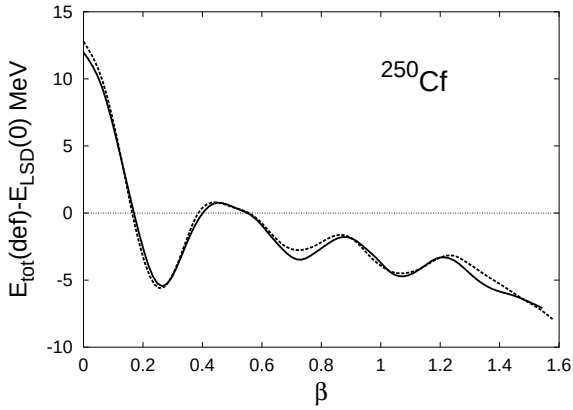

Fig. 4. Total energy relative to the spherical LSD energy obtained along the fission path in the space of the deformation parameters $\{\alpha_{20}, \alpha_{22}, \alpha_{40}, \alpha_{42}, \alpha_{44}\}$ (solid line) and $\{\alpha_{20}, \alpha_{22}, \alpha_{40}\}$ (dashed line).

In conclusion: We have presented the multi-dimensional deformation-space calculation results using a single nucleus as an example; the influence of the higher order multipolarities is less visible in terms of comparison of the energy or deformation curves but has a definite influence on the life-times. On this level of comparisons also the choice of the more modern mean-field parametrisations such as *e.g.* Dirac Woods–Saxon starts playing a non-negligible role. More systematic results will be presented elsewhere.

In particular, the LSD model which includes the effects of the mean-curvature energy influences the final results as expected especially at the highest elongations. For the heavy nuclei this influence is numerically small but systematic and not at all negligible.

Our calculations represent a certain step towards a more precise way to calculate the fission probabilities by taking into account the degrees of freedom that have been usually neglected. Whether such an improvement will be possible without a detailed extension of the formalism to include the new degrees of freedom in the mass parameters is not quite clear at present.

REFERENCES

[1] N. Schunck, J. Dudek, *Acta Phys. Pol. B* **32**, 1103 (2001).

[2] K. Pomorski, J. Dudek, *Phys. Rev.* **C67**, 044316 (2003).

[3] P. Möller, J.R. Nix, W.D. Myers, W.J. Świątecki, *At. Data Nucl. Data Tables* **59**, 185 (1995).

[4] V.M. Strutinsky, *Nucl. Phys.* **A122**, 1 (1968).

[5] D.R. Bes, Z. Szymanski, *Nucl. Phys.* **28**, 42 (1963).